A Connection between Empirical Bond Strength and the Localization of the Electron Density at the Bond Critical Points of the SiO Bonds in Silicates

G. V. Gibbs*

Departments of Geosciences, Materials Science and Engineering, and Mathematics, Virginia Polytechnic Institute and State University, Blacksburg, Virginia 24061

D. F. Cox

Department of Chemical Engineering, Virginia Polytechnic Institute and State University, Blacksburg, Virginia 24061

K. M. Rosso

W.W. Wiley Environmental Molecular Sciences Laboratory, Pacific Northwest National Laboratory, PO Box 999, KB-96, Richland, Washington 99352

Received: June 28, 2004; In Final Form: August 11, 2004

The empirical bond strength of the SiO bond correlates with the value of the electron density at the bond critical point calculated for a large number of silicates and observed for the silica polymorphs stishovite and coesite. The greater the bond strength, the greater the localization of the electron density at the critical point, the shorter the bond, and the greater the covalent character of the bonded interaction. Bond strength and resonance bond number are considered to represent similar properties of the electronic structure of the bond.

The average strength (s) of the MO bonded interactions that comprise an $M^{+z}O_v$ M-cation-containing oxide coordinated polyhedron in a complex ionic crystal was defined by Pauling[1] as $s = +z/v$, where $+z$ is defined to be the formal ionic valence of the M-cation. With this definition, he found the remarkable result that the sum of the bond strengths (ζ) for each of the individual bonded interactions reaching each oxide anion in the structures for a variety of silicates and oxides is exactly equal to 2.0, which is the magnitude of the defined ionic valence of the oxide anion. However, with the discovery that ζ can deviate from 2.0 (in some cases, by as much 40%), Baur[2] found that the observed SiO bond lengths in these cases correlate with ζ, and, as observed earlier by Smith,[3] the larger the value of ζ, the longer the bond. However, with the observation by Pauling[4] that the bond lengths in metals and related materials can be ranked in terms of bond number with a power-law relationship, Brown and Shannon[5] modeled the connection between SiO bond length and SiO bond strength with the power-law expression $s = (R(\mathrm{SiO})/1.625)^{4.5}$, where s is defined to be the empirical bond strength for a given SiO bonded interaction and R(SiO) is the observed bond length. The regression estimates 1.625 and 4.5 were obtained for the individual SiO bond lengths for a large number of silicate structures with the side constraint that the sum of the strengths of the bonded interactions reaching each Si cation and oxyanion in a structure equals their formal valences.

Recently, the theoretical bond critical point (bcp) properties for the electron density distributions[6] generated for the silica polymorphs stishovite[7] and coesite[8] were determined to agree relatively well with those observed. Equally important, model crystal structures for the two polymorphs, together with that for low quartz, which also was generated with first-principles quantum mechanical methods, were determined to agree with those observed,[9−11] with the theoretical bond lengths and angles of the three materials rivaling the accuracy of those determined experimentally (see Table 1 for a comparison of the experimental and theoretical SiO bond lengths and SiOSi angles[7−12]). Theoretical model deformation electron density maps generated for both coesite[8] and stishovite[7,13,14] and $-\nabla^2\rho(\mathbf{r_c})$ isosurface

TABLE 1: Experimental and Theoretical Nonequivalent SiO Bond Lengths and SiOSi Angles for the Silica Polymorphs Stishovite, Low Quartz, and Coesite

	experimental	theoretical
SiO Bond Length (Å)		
stishovite[a]		
equatorial	1.757	1.761
axial	1.808	1.801
low quartz[b]		
	1.612	1.608
	1.613	1.614
coesite[c]		
Si1O1	1.596	1.592
Si1O4	1.613	1.611
Si2O2	1.612	1.610
Si2O4	1.607	1.605
Si1O3	1.614	1.614
Si1O5	1.622	1.621
Si2O3	1.616	1.614
Si2O5	1.620	1.621
SiOSi Bond Angle (°)		
stishovite[a]	130.7	130.6
low quartz[b]	142.4	142.2
coesite[c]		
Si2O2Si2	142.0	141.9
Si1O3Si2	144.2	144.0
Si1O4Si2	149.7	149.1
Si1O5Si2	136.9	136.1

[a] From refs 7 and 11. [b] From refs 9 and 12. [c] From refs 8 and 10.

* Author to whom correspondence should be addressed. E-mail: gvgibbs@vt.edu.

10.1021/jp047202s CCC: $27.50
Published on Web 08/25/2004

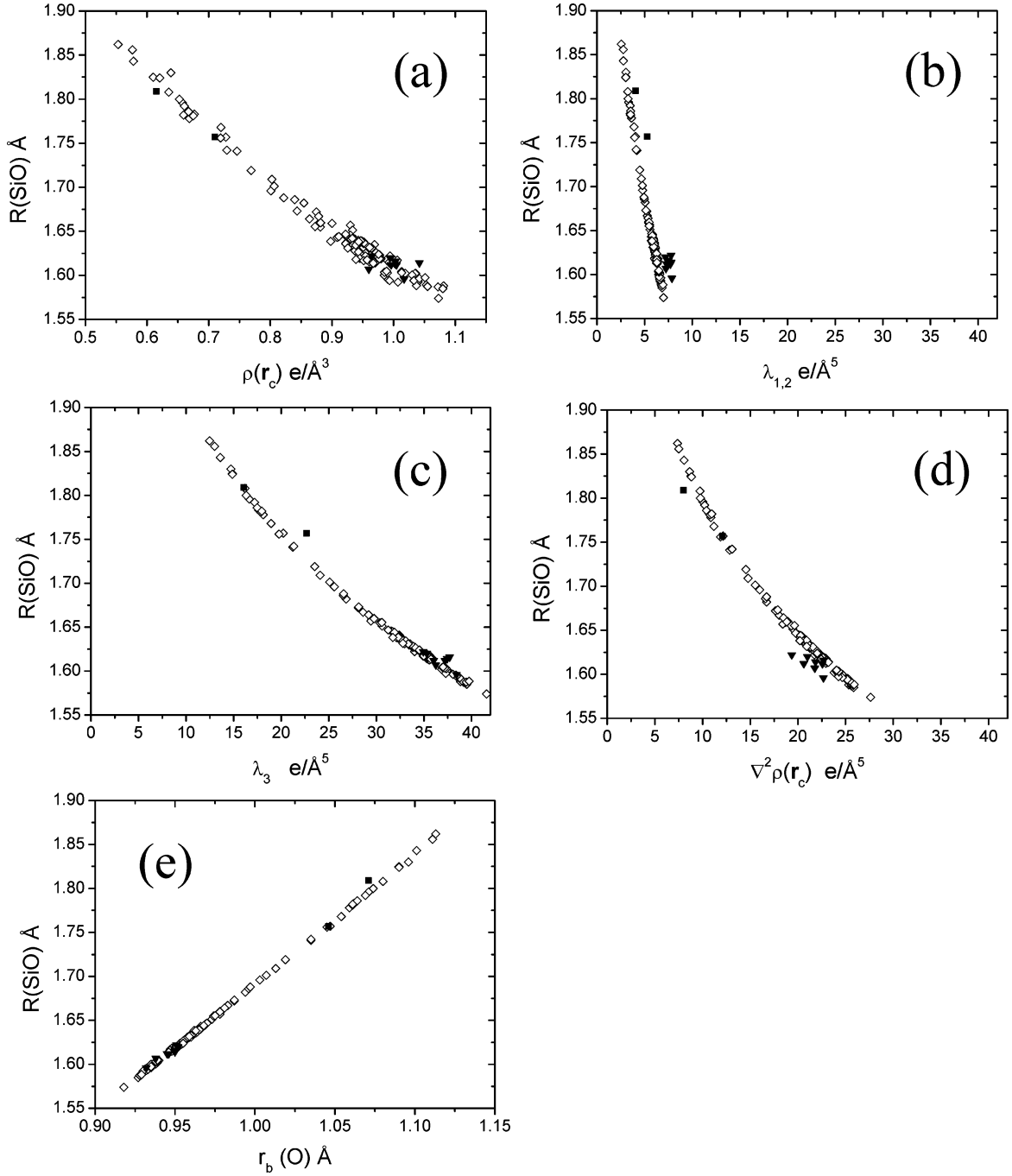

Figure 1. Plot of the observed SiO bond length (R(SiO)) observed for a large number of silicates (denoted by open diamonds, ◇) versus the calculated bond critical point (bcp) properties for the bond:[15] (a) the value of the electron density ($\rho(\mathbf{r_c})$) at the bond critical point; (b) the average of the two curvatures of $\rho(\mathbf{r_c})$ ($\lambda_{1,2}$) measured perpendicular to the bond path, (c) the curvature of $\rho(\mathbf{r_c})$ measured parallel to the bond path in the direction of Si and O, (d) the Laplacian of $\rho(\mathbf{r_c})$, and (e) the bond radius of the oxide anion. The bond length and bcp properties observed for coesite[8] are plotted in the figures as solid triangles (▲), and those for stishovite[7] are plotted as solid squares (■).

maps generated for coesite also agree relatively well with those observed.[8] Furthermore, electron density distributions and the bcp properties have been calculated for the SiO bonded interactions for a large number of silicates, using the local density approximation, Gaussian crystal basis sets, the experimental cell dimensions, and the coordinates of the nonequivalent atoms for each.[15] Scatter diagrams of these data (Figure 1) show that the value of the electron density ($\rho(\mathbf{r_c})$) calculated for the bonded interaction at the bond critical point $\mathbf{r_c}$, along each SiO bond path (see Figure 1a), the average of the two curvatures of $\rho(\mathbf{r_c})$ ($\lambda_{1,2} = (|\lambda_1| + |\lambda_2|)/2$, calculated perpendicular to each path; see Figure 1b), the curvature of $\rho(\mathbf{r_c})$ (λ_3, calculated parallel to each path; see Figure 1c), and the Laplacian of $\rho(\mathbf{r_c})$ ($\nabla^2\rho(\mathbf{r_c})$) (see Figure 1d) each increases as the SiO bond length (R(SiO)) decreases.[15] On the other hand, the bonded radius of the oxide anion (r_b(O)) decreases as the bond length decreases (see Figure 1e). As the electron density is progressively localized at $\mathbf{r_c}$, the SiO bond decreases in length. Concomitant with the localization, the electron density is progressively locally concentrated both perpendicular to the bond path toward $\mathbf{r_c}$ and along the path away from $\mathbf{r_c}$ toward the Si and O atoms, thereby enhancing the shielding of the nuclei of both atoms. Furthermore, the bcp properties determined for multipole representations of the experimental electron density distributions[16−18] for both stishovite and coesite agree with the theoretical values of the SiO bonded interactions, within ∼3%, on average (see Figure 1[8]).

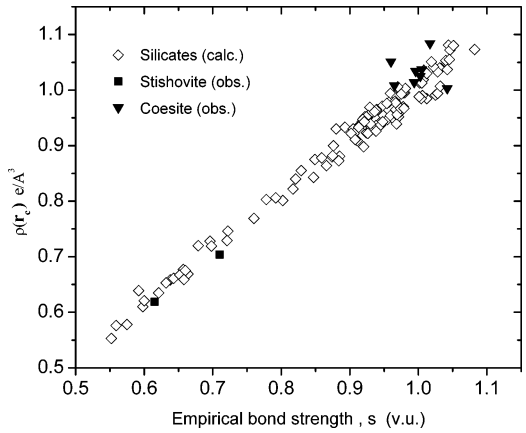

Figure 2. Plot of the value of $\rho(\mathbf{r}_c)$ calculated for the large silicate data set used to prepare Figure 1a (denoted by by open diamonds, ◇) versus the empirical bond strength of each bond (s), where $s = (R(\mathrm{SiO})/1.625)^{4.5}$ and R(SiO) is the observed SiO bond length.[5] The $\rho(\mathbf{r}_c)$ data observed for coesite and stishovite are plotted as solid triangles (▲) and squares (■), respectively, against the s values calculated with the observed bond lengths.

The value of $\rho(\mathbf{r}_c)$ is a measure of the localization of ρ at $\mathbf{r}_c$; therefore, the strength of the SiO bonded interaction is indicated to increase as the length of the bond decreases.

A Connection between Electron Density and Empirical Bond Strength

As noted earlier,[15] a close connection exists between the average value of the Pauling bond strength s and the average theoretical value of $\rho(\mathbf{r}_c)$ for the MO bonded interactions for a large data set of silicates, involving first- and second-row M-cations (M = Li, ..., C; Na, ..., S). A similar connection has also been established between the resonance bond number and the bond strength, with the SiO bond length similarly decreasing with increasing bond number.[19] In this letter, we establish a connection between the $\rho(\mathbf{r}_c)$ values for the SiO bonded interactions displayed in Figure 1 and the empirical SiO bond strength values (s) determined with a power-law expression, based on the observed SiO bond lengths for the silicates.[5]

Empirical bond strengths, which have been calculated for each of the observed SiO bond lengths comprising the large silicate data set, are plotted in Figure 2 against the calculated $\rho(\mathbf{r}_c)$ values used to prepare Figure 1a. The correlation between the two variables is not only well-developed but the regression line has a slope of ~45°. The empirical bond strengths, which have been calculated using the observed bond lengths for stishovite and coesite, are plotted in the figure against the $\rho(\mathbf{r}_c)$ values that have been observed for the two. With the exception of two data points, the experimental data fall within the scatter of the calculated data. Despite the different bases upon which $\rho(\mathbf{r}_c)$ and s are defined, the correlation in Figure 2 indicates that they measure similar properties of the SiO bond: the greater the value of s, the greater the localization of the electron density at the bcp. Because s correlates with R(SiO), it follows that s must not only correlate with $\rho(\mathbf{r}_c)$, as observed in Figure 1a, but also with $\lambda_{1,2}$, λ_3, $\nabla^2\rho(\mathbf{r}_c)$, and r_b(O).

Concluding Remarks

The connection between the empirical bond strength (s) and the electron density at the SiO bond critical point ($\rho(\mathbf{r}_c)$) provides a basis for understanding why the Brown−Shannon bond valence model[5] has been successful in the prediction of inorganic structures and the modeling of defect structures, as well as providing a rationalization for acid−base bonded interactions.[20] Given that the R(SiO) bond critical point (bcp) properties observed for silicates closely parallel the values and trends calculated for representative hydroxyacid silicate molecules,[21] we believe that the trend displayed in Figure 2 applies to the SiO bonded interactions for a variety of similar materials, including siloxane molecules, silicone polymers, silica, and silicate glasses.[22] Finally, because the R(MO) value for first- and second-row M-cations has been determined to correlate with the theoretical values of $\rho(\mathbf{r}_c)$,[15] the connection between s and the bcp properties is expected to hold for the MO bonded interactions for a wide variety of oxide materials.

Acknowledgment. The National Science Foundation (Grant Nos. EAR-9627458 and EAR-0229472), and the Chemical Sciences, Geosciences and Biosciences Division, Office of Basic Energy Sciences, Office of Science, U.S. Department of Energy (Grant DE-FG02-97ER14751) and the U.S. Department of Energy (DE-FG02-03ER15389) are thanked for supporting this study. Professor I. D. Brown at McMasters University and two anonymous reviewers are thanked for critically reading and making several useful recommendations for improving the manuscript.

References and Notes

(1) Pauling, L. *J. Am. Chem. Soc.* **1929**, *51*, 1010−1026.
(2) Baur, W. H. *Trans. Am. Crystallogr. Assoc.* **1970**, *6*, 129−153.
(3) Smith, J. V. *Am. Mineral.* **1953**, *38*, 643−661.
(4) Pauling, L. *J. Am. Chem. Soc.* **1947**, *69*, 542−553.
(5) Brown, I. D.; Shannon, R. D. *Acta Crystallogr., Sect. A: Cryst. Phys., Diffr., Theor., Gen. Crystallogr.* **1973**, *A29*, 266−281.
(6) Bader, R. F. W. *Atoms in Molecules*; Oxford Science Publications: Oxford, U.K., 1990.
(7) Kirfel, A.; Krane, H. G.; Blaha, P.; Schwarz, K.; Lippmann, T. *Acta Crystallogr., Sect. A: Found. Crystallogr.* **2001**, *A57*, 663−677.
(8) Gibbs, G. V.; Whitten, A. E.; Spackman, M. A.; Stimpfl, M.; Downs, R. T.; Carducci, M. D. *J. Phys. Chem. B* **2003**, *107*, 12996−13006.
(9) Gibbs, G. V.; Rosso, K. M.; Teter, D. M.; Boisen, M. B.; Bukowinski, M. S. T. *J. Mol. Struct. (THEOCHEM)* **1999**, *486*, 13−25.
(10) Gibbs, G. V.; Boisen, M. B.; Rosso, K. M.; Teter, D. M.; Bukowinski, M. S. T. *J. Phys. Chem. B* **2000**, *104*, 10534−10542.
(11) Gibbs, G. V.; Cox, D. F.; Ross, N. L. *Phys. Chem. Miner.* **2004**, *31*, 232−239.
(12) Lager, G. A.; Jorgensen, J. D.; Rotella, F. J. *J. Appl. Phys.* **1982**, *53*, 6751−6756.
(13) Spackman, M. A.; Hill, R. J.; Gibbs, G. V. *Phys. Chem. Miner.* **1987**, *14*, 139−150.
(14) Cohen, R. E. First-Principles Theory of Crystalline Silica. In *Silica*; Heaney, P. J., Prewitt, C. T., Gibbs, G. V., Eds.; Reviews in Mineralogy, Vol. 10; Mineralogical Society of America: Washington, DC, 1994; pp 369−402.
(15) Gibbs, G. V.; Boisen, M. B.; Beverly, L. L.; Rosso, K. M. A Computational Quantum Chemical Study of the Bonded Interactions in Earth Materials and Structurally and Chemically Related Molecules. In *Molecular Modeling Theory: Applications in the Geosciences*; Cygan, R. T., Kubicki, J. D., Eds.; Reviews in Mineralogy and Geochemistry, Vol. 42; Mineralogical Society of America: Washington, DC, 2001; pp 345−381.
(16) Stewart, R. F. *Acta Crystallogr., Sect. A: Cryst. Phys., Diffr., Theor., Gen. Crystallogr.* **1976**, *A32*, 565−574.
(17) Hansen, N. K.; Coppens, P. *Acta Crystallogr., Sect. A: Cryst. Phys., Diffr., Theor., Gen. Crystallogr.* **1978**, *A34*, 909.
(18) Stewart, R. F.; Spackman, M. A.; Flensburg, C. *VALRAY User's Manual*, Version 2.1 Edition; Carnegie Mellon University & University of Copenhagen: Pittsburgh, PA, 2000.
(19) Boisen, M. B.; Gibbs, G. V.; Zhang, Z. G. *Phys. Chem. Miner.* **1988**, *15*, 409−415.
(20) Brown, I. D. *The Chemical Bond in Inorganic Chemistry*; Oxford Science Publications: Oxford, U.K., 2002.
(21) Gibbs, G. V.; Boisen, M. B.; Hill, F. C.; Tamada, O.; Downs, R. T. *Phys. Chem. Miner.* **1998**, *25*, 574−584.
(22) Rossano, R.; Farges, F.; Ramos, A.; Delaye, J. M.; Brown, G. E. *J. Non-Cryst. Solids* **2002**, *304*, 167−173.